Vol. 51, No. 12

In Vitro Efficacy of New Antifolates against Trimethoprim-Resistant *Bacillus anthracis*[▽]

Esther W. Barrow,[1] Jürg Dreier,[2] Stefan Reinelt,[2] Philip C. Bourne,[1] and William W. Barrow[1]*

Department of Veterinary Pathobiology, Center for Veterinary Health Sciences, Oklahoma State University, Stillwater, Oklahoma 74078,[1] and Basilea Pharmaceutica, Basel, Switzerland[2]

Bacillus anthracis is innately resistant to trimethoprim (TMP), a synthetic antifolate that selectively inhibits several bacterial dihydrofolate reductases (DHFRs) but not human DHFR. Previously, we were able to confirm that TMP resistance in *B. anthracis* (MIC > 2,048 μg/ml) is due to the lack of selectivity of TMP for the *B. anthracis* DHFR (E. W. Barrow, P. C. Bourne, and W. W. Barrow, Antimicrob. Agents Chemother. 48:4643–4649, 2004). In this investigation, 24 2,4-diaminopyrimidine derivatives, representing a class of compounds with dihydrophthalazine side chains, were screened for their in vitro effects on *B. anthracis* Sterne and their selectivities for the *B. anthracis* DHFR. MICs were obtained by a colorimetric (Alamar blue) broth microdilution assay. Purified human recombinant DHFR (rDHFR) and *B. anthracis* rDHFR were used in a validated enzyme assay to determine the 50% inhibitory concentrations (IC$_{50}$s) and the selectivity ratios of the derivatives. The MICs ranged from 12.8 to 128 μg/ml for all but nine compounds, for which the MICs were ≥128 μg/ml. The IC$_{50}$ values for *B. anthracis* rDHFR ranged from 46 to 600 nM, whereas the IC$_{50}$ values for human rDHFR were >16,000 nM. This is the first report on the in vitro inhibitory actions of this class of antifolates against TMP-resistant *B. anthracis* isolates. The selective inhibition of *B. anthracis* rDHFR and the in vitro activity against *B. anthracis* demonstrate that members of this class of compounds have the potential to be developed into clinically important therapeutic choices for the treatment of infections caused by TMP-resistant bacteria, such as *B. anthracis*.

The increasing incidence of antibiotic-resistant pathogens is a significant threat because of the inability to effectively treat certain infectious diseases. The development of new and efficient antibiotics is an important aspect in dealing with the challenge presented by antibiotic resistance.

Anthrax, although primarily a disease of herbivorous animals, can affect humans as a cutaneous, gastrointestinal, or respiratory disease (12). Respiratory anthrax is a rare disease but difficult to diagnose and fatal in almost all cases unless the patient is treated with antibiotics. The etiological agent of anthrax, *Bacillus anthracis*, is one of the category A priority pathogens on the list of the National Institute of Allergy and Infectious Diseases (NIAID) division of the National Institutes of Health (NIH). One of the objectives of NIH is to develop antimicrobics for use in the treatment of anthrax.

Several antimicrobics, including ciprofloxacin and doxycycline, are approved and available for the treatment of anthrax (14). However, resistance to several of these compounds has been documented (5, 6, 9, 18, 19, 23). In addition, penicillin-resistant *B. anthracis*-like bacteria have been isolated from wild nonhuman primates who died of an anthrax-like disease in Côte d'Ivoire (16).

Both dihydrofolate reductase (DHFR) and dihydropteroate synthase (DHPS) are proven targets for antimicrobial drugs. They play key roles in the folate biosynthetic pathway that generates the cofactors necessary for continued DNA and RNA synthesis. As reported previously, trimethoprim (TMP) and sulfonamides are not effective against *B. anthracis* (1, 20). The genetic basis for TMP and sulfonamide resistance is associated with the chromosomally encoded gene for each enzyme target, DHFR (2) and DHPS (24), respectively. This prompted us to pursue activities for the development of drugs that overcome the TMP resistance of *B. anthracis*. Various antifolates were screened for their in vitro activities against *B. anthracis* and the enzyme target, DHFR. Initial studies with a few of these DHFR inhibitors were reported previously (3). Because of those results, additional derivatives were examined for their effectiveness against *B. anthracis* and the enzyme target, DHFR.

The objectives of the current study were to (i) screen additional inhibitors of *B. anthracis* recombinant DHFR (rDHFR) and to determine the MICs for those that had reasonable in vitro activities (at concentrations <128 μg/ml) and (ii) assay hit compounds to determine the 50% inhibitory concentrations (IC$_{50}$s) for the bacterial and the human enzymes to identify specific antibacterial DHFR inhibitors.

(Parts of this research were presented at the 45th Interscience Conference on Antimicrobial Agents and Chemotherapy, Washington, DC.)

MATERIALS AND METHODS

Microorganisms. *B. anthracis* Sterne was used for initial drug screening. This strain was acquired from Rebecca Morton, Oklahoma State University Center for Veterinary Health Sciences. The *B. anthracis* Ames strain (NR-411) was used for confirmation of activity against a virulent strain and was obtained through the Biodefense and Emerging Infectious Research Resources Repository, NIAID, NIH. Work with the Ames strain was conducted in a CDC-registered and -approved biosafety level 3 laboratory, and appropriate biosafety and security regulations were used. The other strains used in this study included *Enterococcus*
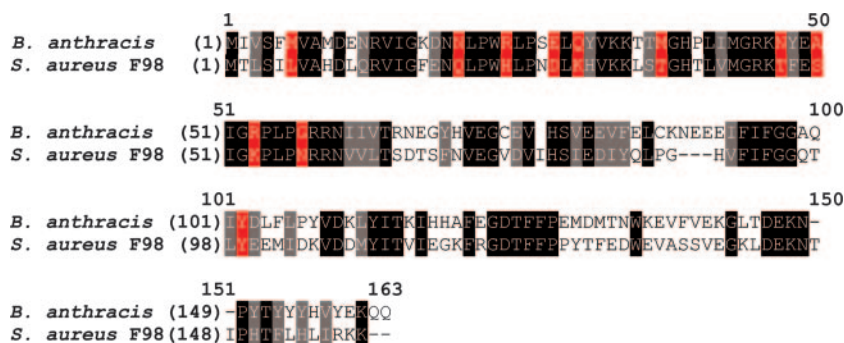

FIG. 1. Alignment of sequences for *B. anthracis* Sterne (GenBank accession number AAT40581) and the F98Y mutant of *S. aureus* ATCC 25923 (10). Sequence identity is indicated by residues highlighted in black, and sequence conservation is indicated by residues highlighted in gray. Residues highlighted in red are located in the active site and are likely to influence inhibitor binding. These residues are discussed in the text in association with the homology model.

faecalis ATCC 29212 and *Escherichia coli* ATCC 25922, which were obtained from ATCC. Upon receipt, the strains were checked for purity and stocks were grown in an appropriate medium.

Compounds. The compounds were provided by Basilea Pharmaceutica, Basel, Switzerland. The compounds were synthesized as described in a previous patent (13).

MIC determinations. The MICs of the compounds for *B. anthracis* Sterne and Ames were determined by an Alamar blue broth microdilution assay, as described previously (3, 4). In the case of the *B. anthracis*, the final inoculum was 5.0×10^4 CFU/ml, equivalent in turbidity to a 0.5 McFarland standard.

Sterile solutions of test and quality control (QC) drugs were maintained at −80°C. The test compounds and the QC drug solutions were prepared at the appropriate concentrations in cation-adjusted Mueller-Hinton broth (Becton Dickinson, Cockeysville, MD) (7) containing 10% Alamar blue and then aliquoted into 96-well plates at 100 µl/well. The plates were prepared and infected on the same day. Doxycycline at three concentrations (twofold dilutions, 1 to 0.25 µg/ml) was used to determine the MIC for *E. coli* ATCC 29255. For plates infected with the Sterne strain, doxycycline was used at 0.0156, 0.03125, and 0.0625 µg/ml. For plates infected with the Ames strain, the doxycycline concentrations at twofold dilutions were 0.0156 to 0.25 µg/ml. TMP-sulfamethoxazole concentrations (twofold dilutions of TMP-sulfamethoxazole from 2/38 to 0.25/4.75 µg/ml) were used for *E. faecalis* ATCC 29212. Sterility control wells and growth control wells for each agent were included in the 96-well plate.

For initial screens of the test compounds, 10-fold dilutions from 128 µg/ml to 0.128 µg/ml were used in triplicate columns. Two columns were infected, and the third column served as a color control. This also allowed observation of drug precipitation. In subsequent panels, drug concentrations were used at twofold dilutions. The MIC for each compound was evaluated four times by using the dilution range of 128 to 0.128 µg/ml. Subsequent MIC evaluations at narrower ranges were also conducted four times. Thus, the MIC for each compound was evaluated eight times in total.

After 16 h incubation, the plates were allowed to equilibrate for 30 min at room temperature before they were sealed with a sterile plate sealer (Nunc). The plate was then read visually and spectrophotometrically in an optical microtiter plate reader programmed to subtract the absorbance at 600 nm from that at 570 nm. The MICs are reported as the lowest drug concentrations yielding a differential absorbance of zero or less (i.e., the color remained blue). The MICs were compared to the acceptable limits for the QC strains (see Table 3 in reference 8) to validate drug performance and medium suitability.

For *B. anthracis* Ames, the drugs which had the best MICs for strain Sterne were prepared in 96-well plates in alternating twofold dilutions to encompass more drug concentrations. QC drugs, as well as sterility and growth control wells, were included as described above. The plates were infected, incubated, and read as described above.

Expression and purification of Sterne rDHFR. The strain Sterne rDHFR was expressed in *E. coli* and purified as described previously (2). Fractions containing purified enzyme were pooled and the His tag was removed by using a Novagen thrombin cleavage kit, according to the manufacturer's instructions. Polyacrylamide gel electrophoresis analysis, performed as described Laemmli (17) with 12.5% acrylamide gels, was used to confirm the cleavage of the His tag and indicated a purity of greater than 95%.

DHFR assay. The activity for Sterne rDHFR was measured at 30°C as the decrease in the absorbance at 340 nm over 3 min (2). The average of two or more determinations was used to determine the IC$_{50}$s.

Homology model. For the generation of the model of the *B. anthracis* DHFR structure, the X-ray structure of the TMP-resistant *Staphylococcus aureus* DHFR F98Y mutant (10) was chosen as a template because the enzyme of this strain shares a relatively high degree of sequence identity (45%) with the *B. anthracis* DHFR. The model was generated with the homology model module of the MOE software package (Chemical Computing Group, Köln, Germany) by using the AMBER 94 force field. The final model is highly similar to the structure of the *S. aureus* DHFR, which is reflected in a root mean square deviation of 0.5 Å (Cα atoms). The sequence used in the DHFR structure paper did not include methionine at position 1 (10). In this study, we have used methionine at position 1, and as a result, F98 is now F99 for the *S. aureus* F98Y mutant (Fig. 1), consistent with the sequence for the parent *S. aureus* ATCC 25923 strain reported previously (11).

RESULTS

Initial screening. In the initial stages, several DHFR inhibitors were tested against *B. anthracis* Sterne, the *B. anthracis* rDHFR, and the human rDHFR. Particularly good results were obtained with four derivatives from one subclass of 2,4-diaminopyrimidine analogues with a dihydrophthalazine side chain (3), referred to here as type A (Table 1).

Encouraged by this finding, we tested more compounds of type A with diverse side chains at the R$_1$ and R$_2$ positions. The results for these additional derivatives are presented in Table 1, along with those for the original four hit compounds (BAL17662, BAL16796, BAL16700, and BAL16763), which are marked in boldface in Table 1. Eight additional derivatives had MICs >128 µg/ml, but the results are not shown in Table 1; they are discussed in the text. We chose 128 µg/ml as the upper MIC with which to conduct the subsequent IC$_{50}$ evaluations with the recombinant enzymes. This was primarily due to the twofold dilution testing range that we used for the initial screening. For compounds with MICs exceeding this value, no IC$_{50}$ determinations were performed. Additionally, all of the compounds listed in Table 1 have very low levels of activity against the human rDHFR.

From the initial screening, it was determined that the best compound was BAL17662, with a MIC of ≤12.8 µg/ml and an IC$_{50}$ for the *B. anthracis* rDHFR of 54 nM (Table 1). This compound also had reduced selectivity for the human rDHFR

TABLE 1. Compounds of type A with MICs of <128 µg/ml for *B. anthracis* Sterne[a]

Compound	R$_1$	R$_2$	Mol wt	MIC (µg/ml) for Sterne (Ames)[b]	IC$_{50}$ (nM)[c]		SR[d]
					BaDHFR	HuDHFR	
E1	-O-CH$_3$	No substitution	444.50	>128	ND	ND	ND
C1	-O-CH$_3$	-CH$_3$	458.52	≤64 (≤64)	92 ± 3.3[e]	>28,000[e]	>304
B2	-O-CH$_3$	-CH$_2$-CH$_3$	472.55	≤32 (≤25.6)	96 ± 14[e]	>27,000[e]	>281
BAL17662	-O-CH$_3$	-CH$_2$-CH$_2$-CH$_3$	486.58	≤12.8 (≤16)	54 ± 12[e]	110,000 ± 26,000[f]	2,037
G1	-O-CH$_3$	-CH$_2$-CH$_2$-CH$_2$-CH$_3$	500.61	≤12.8 (≤12.8)	170 ± 26[e]	>20,000[e]	>118
C2	-O-CH$_3$	-CH$_2$-CH$_2$-CH$_2$-OH	502.58	≤64 (>102.4)	120 ± 9[e]	>25,000[e]	>208
BAL16796	-O-CH$_3$	[structure]	544.61	≤128	300 ± 4[f]	813,000 ± 31,000[f]	2,710
BAL16700	-O-CH$_3$	[structure]	626.30	≤25.6 (>51.2)	46 ± 7[f]	>16,000[f]	>348
C3	-O-CH$_3$	[structure]	512.62	≤25.6 (≤12.8)	200 ± 63[e]	>22,000[e]	>110
D3	-O-CH$_3$	[structure]	526.64	≤12.8 (≤12.8)	260 ± 6[e]	>19,000[e]	>73
A3	-O-CH$_3$	[structure]	534.62	≤64 (≤51.2)	150 ± 13[e]	>19,000[e]	>127
A2	-O-CH$_3$	[structure]	550.62	≤128	97 ± 21[f]	>23,000[f]	>237
B3	-O-CH$_3$	[structure]	582.62	≤128	600 ± 100[f]	>22,000[f]	>37
BAL16763	-O-CH$_3$	[structure]	614.15	≤128	400 ± 13[e]	>42,000[e]	>105
E2	-OH	[structure]	536.60	≤128	69 ± 21[f]	>24,000[f]	>348
G2	[structure]	[structure]	619.73	≤32 (≤25.6)	170 ± 7[e]	>21,000[e]	>124

[a] The chiral center is marked with an asterisk.
[b] MICs are given as the means ± standard errors of the means (*n* = 4).
[c] IC$_{50}$ values are given for the *B. anthracis* DHFR (BaDHFR) and the human (HuDHFR) rDHFR and are means ± standard errors of the mean. ND, not determined.
[d] SR, selectivity ratio, which is the IC$_{50}$ for human DHFR/IC$_{50}$ for *B. anthracis* DHFR.
[e] *n* = 3.
[f] *n* = 2.

(110,000 nM) and a selectivity ratio of 2,037 (Table 1). By grouping this compound with compounds with other, similar structures identified in the first round of testing, i.e., BAL16796, BAL16700, and BAL16763, it is possible to observe the effects of various substituted or unsubstituted alkyl chains at the R_2 position (compounds E1, C1, B2, BAL17662, G1, C2, and BAL16796; Table 1). With no substitution at R_2 (compound E1; Table 1), the in vitro activity is essentially lost (MIC > 128 µg/ml). However, an unsubstituted alkyl chain increases the in vitro activity, as observed with compounds C1, B2, BAL17662, and G1 (Table 1). The optimal length of this side chain remains to be determined. When a hydroxyl group is added to BAL17662, the MIC increases slightly and the IC_{50} increases about twofold (compound C2; Table 1). When a complex substituted alkyl chain is attached (e.g., compound BAL16796), the MIC increases even more (Table 1).

When compounds like BAL16700 and BAL16763 were compared to similar compounds containing cyclic substitutions at the R_2 position (compounds C3, D3, A3, A2, and B3), various effects were observed with this series of 2, 4-diaminopyrimidine analogues. All of these derivatives have MICs of less than 128 µg/ml and a lack of selectivity for the human rDHFR (compounds C3, D3, A3, A2, and B3; Table 1). The best compound in this series is compound D3, in which case the R_2 substitution is cyclohexane. The next best activity is observed with a phenyl group (compound BAL16700) or a cyclopentane group (compound C3) in the R_2 position (Table 1). Addition of a toluene group still maintains good activity and selectivity (compound A3), as does the addition of a phenylmethanol group (compound A2) (Table 1). However, addition of a phenol (compound B1), furan (compound F1), pyridine (compound H1), or 2-phenylethanol group (compound A1) eliminates the in vitro activity (i.e., MIC > 128 µg/ml) (structures not shown). Addition of a 2,4-dimethoxypyrimidine group (compound B3) or an N,N-dimethyl-1-phenylmethanamine group (compound BAL16763) restores reasonable activity and selectivity for the B. anthracis rDHFR (Table 1).

Two other derivatives, not discussed above, that contained modifications at R_1 and R_2 were evaluated. Compound E2, with a hydroxyl group at R_1 and a phenylmethanol group at R_2, has a MIC less than 128 µg/ml and an IC_{50} of 69 µg/ml (Table 1). Compound G2, which is similar to compound BAL16700 but with a 2′-morpholinoethoxy group at R_1, has a MIC of ≤32 µg/ml (Table 1).

Other derivatives that were not highly active in vitro (i.e., MICs > 128 µg/ml) included the indicated substitutions for R_1 and R_2, respectively, as follows: compound D1, hydroxyl and phenol; compound D2, dimethoxymethyl and phenol; compound F2, dimethoxymethyl and phenylmethanol; and compound H2, methyl 2-methoxyacetyl and phenol.

Evaluation of B. anthracis Ames. For these evaluations, the drug concentration ranges were customized on the basis of previous results obtained with the Sterne strain. The MICs for these 10 compounds are given in parentheses after the MICs reported for the Sterne strain in Table 1. Essentially, there were no marked differences for compounds C1, B2, BAL17662, G1, C3, D3, A3, and G2 (Table 1). However, compounds C2 and BAL16700 (Table 1) showed marked increases in their MICs for the Ames strain. The reason for this was not examined further.

Homology model. We have generated a model of the B. anthracis DHFR structure to rationalize our experimental results and to subsequently optimize our inhibitors. As discussed previously, an X-ray structure of the TMP-resistant S. aureus F98Y DHFR mutant was selected as a template. The sequence alignments for these two proteins are shown in Fig. 1, along with the residues discussed here (highlighted in red). It should be noted that the similarity of the sequence of the strain Sterne DHFR is 100% with the sequences of the DHFRs of several virulent strains of B. anthracis, including the Ames strain (2). As the F99Y mutation causes TMP resistance in S. aureus (10), it appears likely that the corresponding tyrosine is also involved in the TMP resistance of B. anthracis (102Y) (Fig. 2). As expected by the sequence similarity, the model obtained is highly similar to the template structure, which is reflected in a root mean square deviation of 0.5 Å for the Cα atoms. Also, for the majority of the side chains in the inhibitor-binding pocket, an almost identical position is assigned.

However, several deviations which are likely to influence the binding of inhibitors can be observed (Fig. 2). In B. anthracis, a methionine is located at the position of the L6 of S. aureus. This alteration can be expected to have a negative influence on the inhibitor affinity, since this residue contributes to the shape of the subpocket hosting the diamino-pyrimidine moiety. The change of D28 (in S. aureus) to a glutamate is expected to result in a significant weakening of the inhibitor affinity (Fig. 2). A shift of the inhibitor of at least 0.5 Å is required to maintain the hydrogen bonding. Three mutations are observed in the proximity of the dimethoxy-phenyl moiety. The mutation of T47 to an asparagine residue (Fig. 2) not only decreases the size of this subpocket but also alters the donor-acceptor pattern (Fig. 2). Although the mutations of Q20 to an asparagine and especially of the mutation of S50 to an alanine (Fig. 1, and 2) are located at the edge of the binding pocket, they can be expected to influence significantly the preference for R_1 substituents, as both the shape and the hydrogen-bond donor-acceptor pattern are considerably changed.

In contrast to the change of N57G, the mutation K30Q (Fig. 1 and 2) appears to be more relevant since it renders this residue into a potential hydrogen-bond partner for substituents at the R_2 position. An indirect effect might be caused by the mutation of T37 to a methionine (Fig. 1 and 2). This residue is involved in a hydrogen-bonding pattern, which fixes the position of R59 in the S. aureus DHFR. A weakening of this H-bond pattern can result in an alternative conformation of the arginine, which would significantly decrease the size of this subpocket.

The preference for R_1 and R_2 substituents might also be influenced by the mutations of H24 and K53 to arginine residues (Fig. 1). The modeled orientations of folate and TMP in the binding pocket of the B. anthracis DHFR homology model are shown in an electrostatic surface representation in Fig. 3. The pteridine ring of the folate is buried inside the negatively charged pocket, with the glutamate moiety protruding out from the pocket, where its position is stabilized by a positively charged surface patch formed by the side chains of arginine residues R24, R53, and R58, together with lysine residues K34 and K111. The change of both the size and the donor and acceptor properties of this positively charged patch that forms the ceiling and left wall of the entrance to the folate-binding
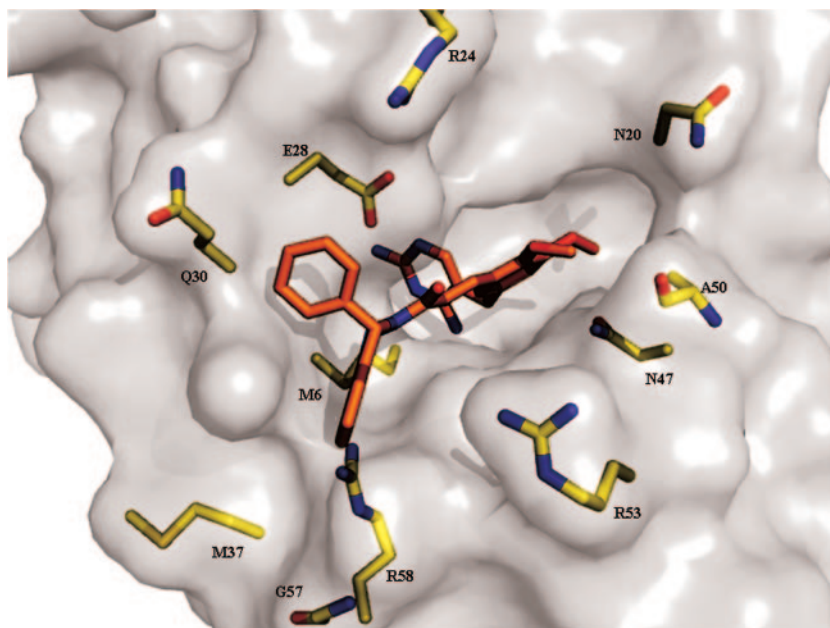
FIG. 2. View of the binding pocket of a modeled *B. anthracis* DHFR-phthalazine inhibitor complex. The highlighted amino acid side chains are different from the amino acids in the *S. aureus* enzyme and are expected to influence inhibitor binding.

pocket could result in additional H-bond interactions. However, due to the high solvent exposure of these residues, this hypothesis requires further investigation either by structure analysis of the *B. anthracis* DHFR or by mutation experiments.
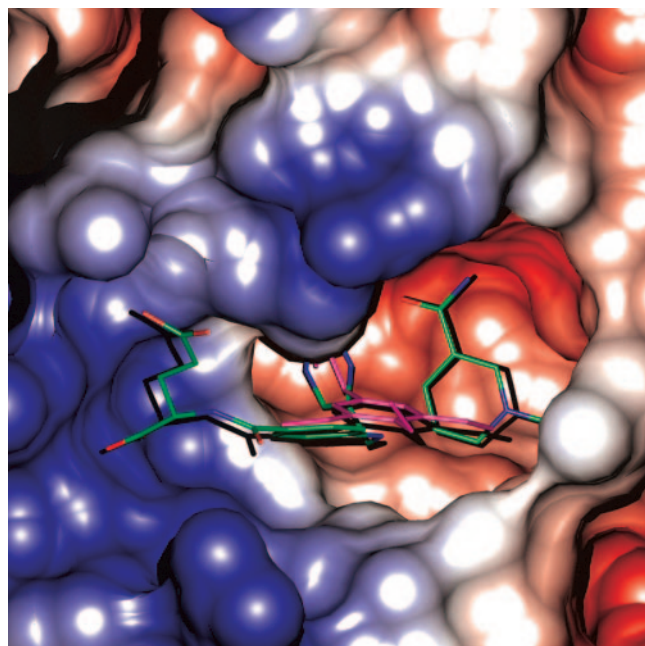

FIG. 3. Electrostatic surface representation of the folate-binding pocket in the *B. anthracis* homology model. The surface is color coded from negative red (^-V_e) to positive blue (^+V_e). The binding positions of folate and NADPH are shown as a stick representation. The modeled binding position of TMP is shown as a magenta stick representation. The positively charged area that forms a binding pocket for large R_2 groups can be seen clearly at the bottom. The figure was generated with the CCP4MG program (21).

DISCUSSION

In 2005, we reported on a group of 2,4-diaminopyrimidine derivatives with in vitro activities against *B. anthracis* Sterne and selective activities against *B. anthracis* rDHFR but not human rDHFR (3). For five of the six derivatives, the MICs ranged from 12.5 to 128 µg/ml (3). The IC_{50} values for the *B. anthracis* rDHFR ranged from 46 to 404 nM for four compounds, while the IC_{50} values for human rDHFR were greater than 16,000 nM, with the best being 813,000 nM (3). To our knowledge, this was the first such report demonstrating any antifolate with activity against *B. anthracis*.

Recently, Joska and Anderson reported on several 2,4-diamino-5-deazapteridine and pyrimidine derivatives with in vitro activities against *Bacillus cereus* (15). The most potent compound was in the 2,4-diamino-5-deazapteridine group, with an MIC_{50} of 1.6 µg/ml (15). Using recombinant *B. cereus* DHFR (which has 98% sequence identity with the *B. anthracis* DHFR), the investigators were able to show IC_{50}s ranging from 0.27 to 252 µM (i.e., 270 to 252,000 nM) (15); no comparative evaluation was reported for human DHFR. However, the authors did cite previous data obtained with some of the compounds for rat DHFR in which the IC_{50} was 25 µM for the best compound (22); that compound had a MIC_{50} of 2.6 µg/ml (15). The six pyrimidine derivatives were much less selective for the *B. cereus* rDHFR, with IC_{50}s ranging from 37 to 150 µM. Apparently, none of the antifolates in the Joska and Anderson study were evaluated against an avirulent or virulent strain of *B. anthracis* (15).

In our current investigation we have extended the findings of our previous studies with the 2,4-diaminopyrimidine group of antifolates. Additionally, the in vitro activities of several of the hit compounds have been confirmed with the virulent Ames strain. The most active compounds have small, hydrophobic side chains at positions R_1 and R_2 (e.g., compounds BAL17662, B2,

and BAL16700; Table 1). It appears that the side chain at position R_2 should be larger than a methyl or ethyl group for optimal activity (Table 1). A molecule without a side chain at position R_2 and a methoxy group at position R_1 is inactive against *B. anthracis* Sterne (e.g., compound E1; Table 1). Adducts larger than cyclohexane show reduced activities, probably because of steric problems but also because of electronic properties (e.g., compounds A1, A2, B1, B3, and BAL16763 versus compound BAL16700; Table 1). A benzyl side chain is well tolerated, while a pyridine leads to a loss of activity of the molecule (e.g., compound H1 versus compound BAL16700; Table 1). Compounds with a methoxy group at position R_1 have antibacterial activities similar to that of a compound with a 2'-morpholino-ethoxy side chain at the same position (e.g., compound G2 versus compound BAL16700; Table 1). This indicates a flexibility for side chains at R_1 which can be further exploited.

These results are in line with those obtained with the *B. anthracis* DHFR homology model developed on the basis of the crystal structure of the DHFR from a TMP-resistant *S. aureus* strain (10). For example, the different IC_{50} values of compounds G1, C2, and BAL16796 reflect well the expected alteration of the preference for substituents at position R_2. Of these three compounds, compound BAL16796 showed the best affinity and compound C2 showed the poorest affinity in *S. aureus* (data not shown). According to molecular modeling, this ranking is changed in *B. anthracis* due to the favorable interactions of the hydroxyl group of compound C2 and the repulsive interactions of the carbonyl group of compound BAL16796 with the Q30 (which replaced the K30 of *S. aureus*), thus rendering compound C2 a better inhibitor than compound BAL16796 of the *B. anthracis* DHFR (Table 1).

The model also helped to identify several residues which are likely to contribute to the altered ligand-binding properties of the *B. anthracis* DHFR. The mutations D28E and L6M appear to affect mainly the diaminopyridine scaffold of the inhibitors, whereas other mutations, in particular, S50A, K30Q, and T37M, are likely to influence the selectivity for the R_1 and R_2 substituents.

The data obtained in this study show that the DHFR inhibitors tested have the potential to become clinically relevant drugs. Optimization of the MIC, while keeping the excellent selectivity for the bacterial enzyme, is a next goal. A chemistry program will be guided by structural information to make the proper modifications. The development of effective antimicrobials affecting this target in *B. anthracis* is particularly important for the treatment of anthrax. Such a drug would generally be welcomed as a contribution to address the problem of infections caused by antibiotic-resistant bacteria.

ACKNOWLEDGMENTS

REFERENCES

1. **Bakici, M. Z., N. Elaldi, M. Bakir, I. Dodmetas, M. Erandac, and M. Turan.** 2002. Antimicrobial susceptibility of *Bacillus anthracis* in an endemic area. Scand. J. Infect. Dis. **34:**564–566.
2. **Barrow, E. W., P. C. Bourne, and W. W. Barrow.** 2004. Functional cloning of *Bacillus anthracis* DHFR and confirmation of natural resistance to trimethoprim. Antimicrob. Agents Chemother. **48:**4643–4649.
3. **Barrow, E. W., J. Dreier, and W. W. Barrow.** 2005. Selective inhibitors for anthrax, abstr. F-2072. Abstr. 45th Intersci. Conf. Antimicrob. Agents Chemother. American Society for Microbiology, Washington, DC.
4. **Barrow, E. W., M. W. Valderas, P. C. Bourne, and W. W. Barrow.** 2006. Newly developed colorimetric drug screening assay for *Bacillus anthracis*. Int J. Antimicrob. Agents **27:**178–180.
5. **Brook, I., T. B. Elliott, H. I. Pryor, T. E. Sautter, B. T. Gnade, J. H. Thakar, and G. B. Knudson.** 2001. In vitro resistance of *Bacillus anthracis* Sterne to doxycycline, macrolides and quinolones. Int. J. Antimicrob. Agents **18:**559–562.
6. **Cavallo, J. D., F. Ramisse, M. Girardet, J. Vaissaire, M. Mock, and E. Hernandez.** 2002. Antibiotic susceptibilities of 96 isolates of *Bacillus anthracis* isolated in France between 1994 and 2000. Antimicrob. Agents Chemother. **46:**2307–2309.
7. **CLSI.** 2006. Methods for dilution antimicrobial susceptibility tests for bacteria that grow aerobically; approved standard vol. 26. CLSI, Wayne, PA.
8. **CLSI.** 2006. Performance standards for antimicrobial susceptibility testing; sixteenth informational supplement 26. CLSI, Wayne, PA.
9. **Coker, P. R., K. L. Smith, and M. E. Hugh-Jones.** 2002. Antimicrobial susceptibilities of diverse *Bacillus anthracis* isolates. Antimicrob. Agents Chemother. **46:**3843–3845.
10. **Dale, G. E., D. Broger, A. D'Arcy, P. G. Hartman, R. DeHoogt, S. Jolidon, I. Kompis, A. M. Labhardt, H. Langen, H. Locher, M. G. Page, D. Stüber, R. L. Then, B. Wipf, and C. Oefner.** 1997. A single amino acid substitution in *Staphylococcus aureus* dihydrofolate reductase determines trimethoprim resistance. J. Mol. Biol. **266:**23–30.
11. **Dale, G. E., R. L. Then, and D. Stuber.** 1993. Characterization of the gene for chromosomal trimethoprim-sensitive dihydrofolate reductase of *Staphylococcus aureus* ATCC 25923. Antimicrob. Agents Chemother. **37:**1400–1405.
12. **Dixon, T. C., M. Meselson, J. Guillemin, and P. C. Hanna.** 1999. Anthrax. N. Engl. J. Med. **341:**815–826.
13. **Guerry, P., S. Jolidon, R. Masciadri, H. Stalder, and R. Then.** May 1996. Novel benzyl pyrimidines. Switzerland patent PTC Int. Appl. WO 96/16046.
14. **Inglesby, T. V., D. A. Henderson, J. G. Bartlett, M. S. Ascher, E. Eitzen, A. M. Friedlander, J. Hauer, J. McDade, M. T. Osterholm, T. O'Toole, G. Parker, T. M. Perl, P. K. Russell, and K. Tonat.** 1999. Anthrax as a biological weapon. JAMA **281:**1735–1745.
15. **Joska, T. M., and A. C. Anderson.** 2006. Structure-activity relationships of *Bacillus cereus* and *Bacillus anthracis* dihydrofolate reductase: toward the identification of new potent drug leads. Antimicrob. Agents Chemother. **50:**3435–3443.
16. **Klee, S. R., M. Ozel, B. Appel, C. Boesch, H. Ellerbrok, D. Jacob, G. Holland, F. H. Leendertz, G. Pauli, R. Grunow, and H. Nattermann.** 2006. Characterization of *Bacillus anthracis*-like bacteria isolated from wild great apes from Cote d'Ivoire and Cameroon. J. Bacteriol. **188:**5333–5344.
17. **Laemmli, U. K.** 1970. Cleavage of structural proteins during the assembly of the head of bacteriophage T4. Nature **227:**680–685.
18. **Lalitha, M. K., and M. K. Thomas.** 1997. Penicillin resistance in *Bacillus anthracis*. Lancet **349:**1522.
19. **Mohammed, M. J., C. K. Marston, T. Popovic, R. S. Weyant, and F. C. Tenover.** 2002. Antimicrobial susceptibility testing of *Bacillus anthracis*: comparison of results obtained by using the National Committee for Clinical Laboratory Standards broth microdilution reference and Etest agar gradient diffusion methods. J. Clin. Microbiol. **40:**1902–1907.
20. **Odendaal, M. S., P. M. Pieterson, V. deMos, and A. D. Botha.** 1991. The antibiotic sensitivity patterns of *Bacillus anthracis* isolated from the Kruger National Park. Onderstepoort J. Vet. Res. **58:**17–19.
21. **Potterton, L., S. McNicholas, E. Krissinel, J. Gruber, K. Cowtan, P. Emsley, G. N. Murshudov, S. Cohen, A. Perrakis, and M. Noble.** 2004. Developments in the CCP4 molecular-graphics project. Acta Crystallogr. D Biol. Crystallogr. **60:**2288–2294.
22. **Rosowsky, A., R. A. Forsch, and S. F. Queener.** 2003. Further studies on 2,4-diamino-5-(2',5'-disubstituted benzyl)pyrimidines as potent and selective inhibitors of dihydrofolate reductases from three major opportunistic pathogens of AIDS. J. Med. Chem. **46:**1726–1736.
23. **Stephenson, J.** 2002. Experts focus on infective agents of bioterrorism. JAMA **287:**575–576.
24. **Valderas, M. W., P. C. Bourne, and W. W. Barrow.** 2007. Genetic basis for sulfonamide resistance in *Bacillus anthracis*. Microb. Drug Resist. **13:**12–21.